Numerical Analysis of Curved Embankment of an Upstream Tailings Dam

Linda Ormann
Geotechnical Engineer, SWECO Infrastructure AB, Gjörwellsgatan 22, Stockholm, Sweden
e-mail: linda.ormann@sweco.se

Muhammad Auchar Zardari
Ph.D student, Department of Civil, Environmental and Natural Resources Engineering, Luleå University of Technology, Luleå, Sweden
e-mail: muhammad.zardari@ltu.se

Hans Mattsson
Assistant Professor, Department of Civil, Environmental and Natural Resources Engineering, Luleå University of Technology, Luleå, Sweden
e-mail: hans.mattsson@ltu.se

Annika Bjelkevik
Geotechnical Engineer, SWECO Infrastructure AB, Gjörwellsgatan 22, Stockholm, Sweden
e-mail: annika.bjelkevik@sweco.se

Sven Knutsson
Professor, Department of Civil, Environmental and Natural Resources Engineering, Luleå University of Technology, Luleå, Sweden
e-*mail: sven.knutsson@ltu.se*

ABSTRACT

A curved embankment (corner) of an upstream tailings dam was analyzed with the finite element method to identify possible zones of low compressive stresses susceptible to hydraulic fracturing that might initiate internal erosion. The embankment was also analyzed as a straight section, with the same cross section as in the corner, in order to compare compressive stresses in the corner and the straight section. The analysis showed that in comparison to the straight section of the dam, the compressive stresses in the corner were (*i*) much lower above the phreatic level, in the rockfill banks and the filter zones, and (*ii*) fairly lower below the phreatic level. The rockfill and the filter contain coarse materials, which are not sensitive to hydraulic fracturing and internal erosion. An increase in radius of the corner is proposed to avoid too low compressive stresses that may develop due to future raisings. The slope stability analysis showed that the corner is currently stable, but an additional rock fill bank on the downstream toe is required for future raisings.

KEYWORDS: tailings dams, curved embankments, cracks, internal erosion, hydraulic fracturing, slope stability.

INTRODUCTION

A case study of a finite element analysis of an upstream tailings dam named Aitik, located in the north of Sweden, is presented. This study investigates the potential risk of hydraulic fracturing followed by internal erosion in the corner between the dam sections E-F and G-H (Figure 1). The corner E-F/G-H can be considered as a curved embankment in which retained tailings exert lateral earth pressure on the inner side of the embankment. Consequently, low compressive stresses (and even tensile stresses) may develop near the surface along the outer side of the embankment. Thus, the zones of low compressive stresses in the corner may be sensitive to hydraulic fracturing and internal erosion.

In embankments, cracks or weak zones can appear even at very small tensile stresses. If no cracks develop immediately due to small deformations, cracking may occur later by hydraulic fracturing (Sherard, 1986; Kjaernsli *et al.*, 1992). Internal erosion can then initiate through these cracks. Hydraulic fracturing in an embankment dam may occur through the zones of low compressive stresses, i.e. along the plane of minor effective principal stress (Kjaernsli *et al.*, 1992). Hydraulic fracturing due to high water pressures might have caused leakage or failure of many embankment dams (Sherard, 1986; Singh and Varshney, 1995).

Recently in Hungary, on October 4, 2010, Ajka tailings pond failed at a corner section. In this incident, 0.6 million cubic meters of sludge was released, which killed ten and injured 120 people (WISE, 2010). The possible causes of the failure of Ajka tailings pond were (*i*) generation of excess tensile stresses in the corner, and (*ii*) differences in cross sections of the two dikes that formed the corner (Zanbak, 2010).

In a report (SWECO, 2005), it has been mentioned that low compressive stresses (and tensile stresses) might arise at the corner E-F/G-H. Since then, the dam has been raised, and the corner has become sharper.

In this paper, the corner E-F/G-H was analyzed with the finite element program PLAXIS 2D (Brinkgreve, 2002) in order to locate the zones of low compressive stresses that may be susceptible to hydraulic fracturing and internal erosion. The results of this study have been previously published in a report (Ormann and Bjelkevik, 2009).

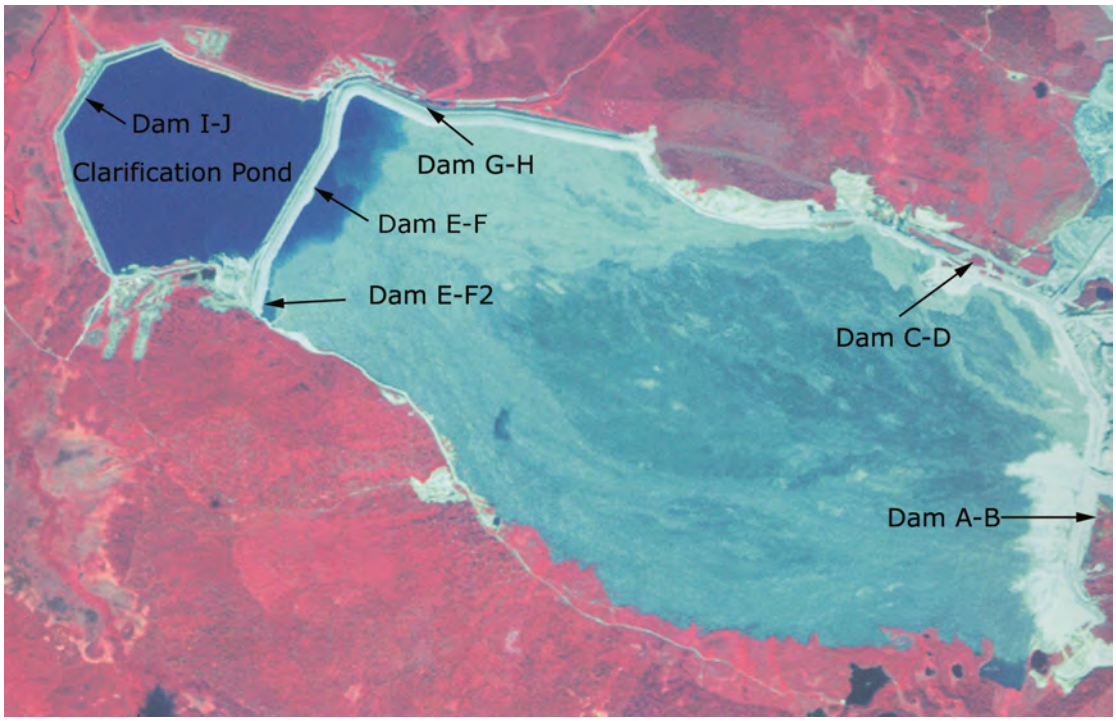

Figure 1: Aerial view of Aitik tailings dam and impoundment (Photo courtesy of Boliden Mineral AB).

FINITE ELEMENT MODEL

The stability of the corner E-F/G-H was analysed with PLAXIS 2D, which is a finite element program for numerical analysis of geotechnical structures. The corner represents a complex three-dimensional geometry. An axisymmetric condition was assumed to model this geometry in two-dimensional space. This condition can be used for circular structures with an almost uniform cross section with load distribution around the central axis. In an axisymmetric condition, the *x*-coordinate represents the radius, and the *y*-coordinate denotes the axial line of symmetry.

It is previously mentioned that due to horizontal pressure of retained tailings at the inner side of the corner, too low compressive stresses may occur near the surface along the outer side of the corner. It is assumed that if the corner is straightened, then the compressive stresses may be sufficiently high to resist hydraulic fracturing and internal erosion. Therefore, it is important to compare the compressive stresses in the corner with the straight section of the dam. Hence, the corner was also modelled with a plane strain condition, which is appropriate for any geotechnical structure - whose length is large compared with its cross section. Figure 2 illustrates the difference between a plane strain and an axisymmetric condition (Brinkgreve, 2002). In this paper, the compressive stresses are taken as positive and the tensile stresses as negative.

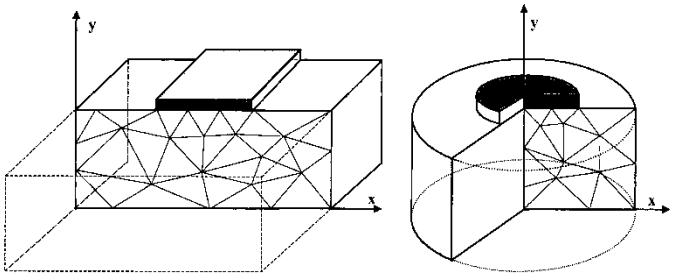

Figure 2: (*a*) Plane strain condition, and (*b*) Axisymmetric condition (Brinkgreve *et al.*, 2010).

It has been assumed that the stored tailings and the dam are raised 3 meter per year starting from the level 376 m above mean sea level. The crest level of the dam is 2 m above the level of the stored tailings. The present crest level of the dam in year 2010 is 387 m. The cross section of the corner is shown in figure 3. The estimated radius is 195 m (Figure 4). It is supposed that the dam is to be raised in stages with the upstream construction method with side slope of 1:6 (vertical to horizontal). Each stage comprises a raising phase of 10 days and a consolidation phase of 355 days.

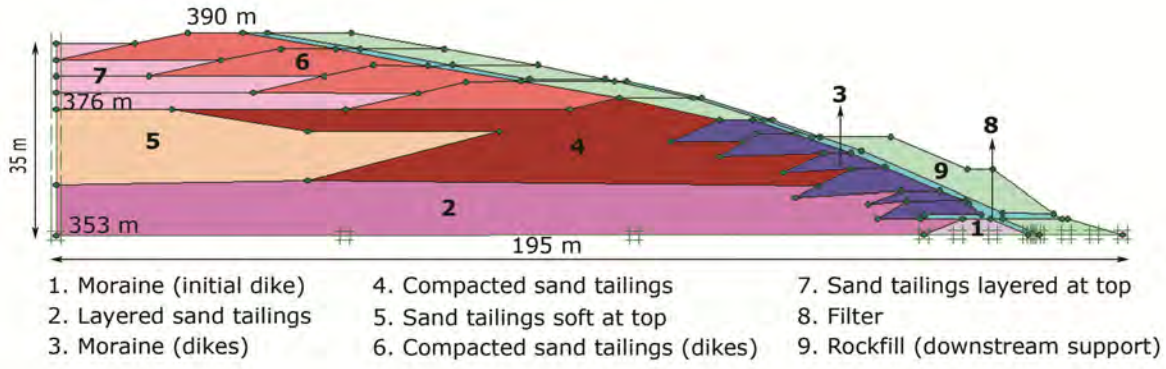

Figure 3: Cross section of corner E-F/G-H.

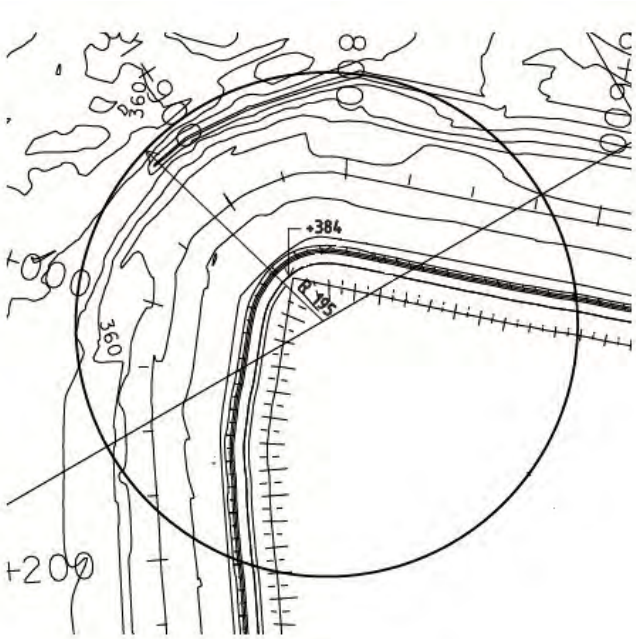

Figure 4: Plan of existing corner between the dam sections E-F and G-H. The radius is 195 m.

The finite element model of the corner is presented in figure 5. The finite element mesh in each cluster is composed of 15 node triangular elements. The computations were initially performed with different levels of coarseness of the mesh (fine, and very fine). There was a small difference in the results from the computations done with the fine and the very fine mesh. Therefore, the fine mesh was used in the analysis to save computational time. The horizontal displacements are assumed to be zero along the left vertical boundary. A fixed base was used assuming that the bottom of the dam lies on a dense and impervious moraine deposit. Water flow can occur through all boundaries in the geometry, except at the left vertical boundary and the base.

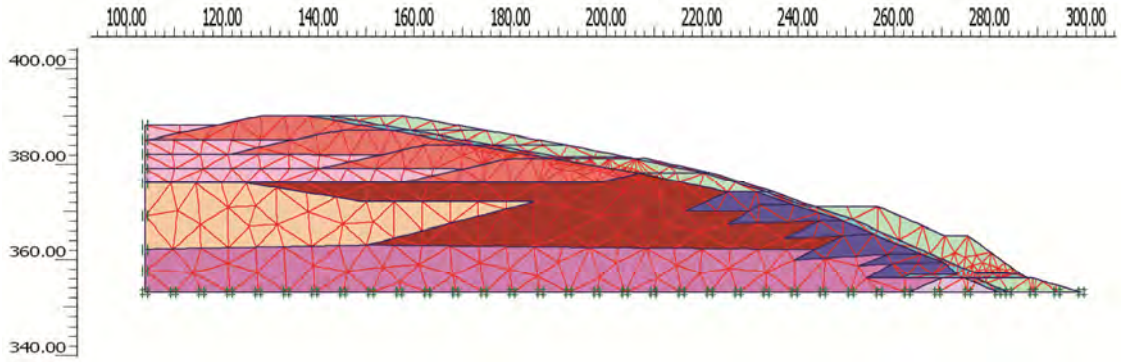

Figure 5: Finite element mesh of corner E-F/G-H.

The Mohr-Coulomb (MC) model was applied to all the materials (tailings, rockfill, and filter) in the dam. The MC model is a simple elastic - plastic model, which contains five model parameters that can be easily determined from laboratory tests. The parameters of the MC model (except Poisson's ratio and angle of dilatancy), were evaluated from field and

laboratory tests, and are presented in Table 1 (Jonasson, 2007; Pousette, 2007; Jonasson, 2008). The Poisson's ratio is assumed to be 0.33 for all the materials, which is a representative value for this type of analysis (Brinkgreve, 2002). The angle of dilatancy of each material is assumed to be zero, which is a convenient assumption for loose and contractant soil e.g. tailings that occupy the major portion of the dam.

The undrained shear strength of loose tailings was determined from direct shear tests. The failure was evaluated at 0.15 % of shear strain (SGF, 2004). The undrained shear strength results were in agreement with the MC model predictions. Therefore, in this case it can be interpreted that the undrained shear strength of loose tailings is not over predicted with the MC model, which generally over estimates the undrained shear strength of normally consolidated clays (Brinkgreve, 2005).

As mentioned earlier, the possible risks of hydraulic fracturing followed by internal erosion in the corner have been investigated in this study. The hydraulic fracturing can occur along the plane of the minor effective principal stress. Therefore, it is important to locate the position of the minor effective principal stress in the corner. In this connection, consolidation analysis was performed for staged construction of the dam. The minor effective principal stress was calculated from the results of the consolidation analysis. In addition to this, safety analysis was also carried out to determine the slope stability of the dam.

Table 1: Parameters of the Mohr-Coulomb model (Jonasson, 2007; Pousette, 2007; Jonasson, 2008)

Material type	γ_{unsat} (kN/m^3)	γ_{sat} (kN/m^3)	k_x (m/s)	k_y (m/s)	E (kN/m^2)	c' (kN/m^2)	φ' (º)
Moraine (initial dike)	20	22	9.95×10^{-8}	4.98×10^{-8}	20000	1	35
Layered sand tailings	17	18.5	5.5×10^{-7}	5.56×10^{-8}	9312	9.5	22
Moraine (dikes)	20	22	4.98×10^{-8}	1×10^{-8}	20000	1	37
Compacted sand tailings	16	19	1×10^{-6}	9.95×10^{-8}	8790	13	26
Sand tailings soft at top	18	18	9.95×10^{-8}	1×10^{-8}	3048	6	18
Compacted sand tailings (dikes)	16	19	1×10^{-6}	9.95×10^{-8}	7200	13	26
Sand tailings layered at top	17	18.5	5.5×10^{-7}	5.56×10^{-8}	3895	9.5	22
Filter	18	20	1×10^{-3}	1×10^{-3}	20000	1	32
Rockfill (downstream support)	18	20	1×10^{-1}	1×10^{-1}	40000	1	42

Note: γ_{unsat} is the unit weight above phreatic level, γ_{sat} is the unit weight below phreatic level, k_x is the hydraulic conductivity in horizontal direction, k_y is the hydraulic conductivity in vertical direction, E is the Young's modulus, c' is the effective cohesion and φ' is the effective friction angle.

FINITE ELEMENT ANALYSIS

Evaluation of minor effective principal stress

An element of a soil under an embankment can be subjected to three principal stresses acting on three mutually perpendicular planes. For the geometry of the corner E-F/G-H, two of the principal stresses act in the *x-y* plane, and the third principal stress occurs in the *z* direction along the length of the dam. Hence, the normal effective stress σ'_{zz} in the *z* direction is also a principal stress. The major effective principal stress σ'_1 and the minor effective principal stress σ'_2 in the *x-y* plane can be calculated according to Das (1997):

$$\sigma'_{1,2} = \frac{1}{2}\left(\sigma'_x + \sigma'_y\right) \pm \sqrt{\left(\frac{\sigma'_x + \sigma'_y}{2}\right)^2 + \tau_{xy}^2} \qquad (1)$$

where σ'_x and σ'_y are the effective normal stress components in the *x* and *y* directions respectively, and τ_{xy} is the shear stress component in the *x-y* plane. The values of these stress components were directly obtained from the results of the finite element analysis of the corner.

The major effective principal stress occurred in the *x-y* plane. As stated earlier, for this analysis, it is essential to locate the minor effective principal stress in the three dimensional space. Therefore, the minor effective principal stress σ'_2 in the *x-y* plane was compared to the effective normal stress σ'_{zz} in the *z* direction. Figure 6 illustrates the ratio σ'_{zz} / σ'_2 of the effective normal stress in the *z* direction and the minor effective principal stress in the *x-y* plane. If the ratio is less than one, the effective normal stress in the *z* direction is the minor effective principal stress in the three dimensional space. In the upper parts of the geometry, the effective normal stress in the *z* direction, dominates as the minor effective principal stress in the three dimensional space. When the ratio is equal to one, the minor effective principal stress in the *x-y* plane and the effective normal stress in the *z* direction are equal. If the ratio is greater than one, the minor effective principal stress in the *x-y* plane acts as the minor effective principal stress in the three dimensional space. The ratio of 1 to 1.2 indicates that the effective normal stress in the *z* direction is approximately of the same magnitude as the minor effective principal stress in the *x-y* plane. It is obvious that the minor effective principal stress in the three dimensional space is located either in the *x-y* plane or in the *z* direction.

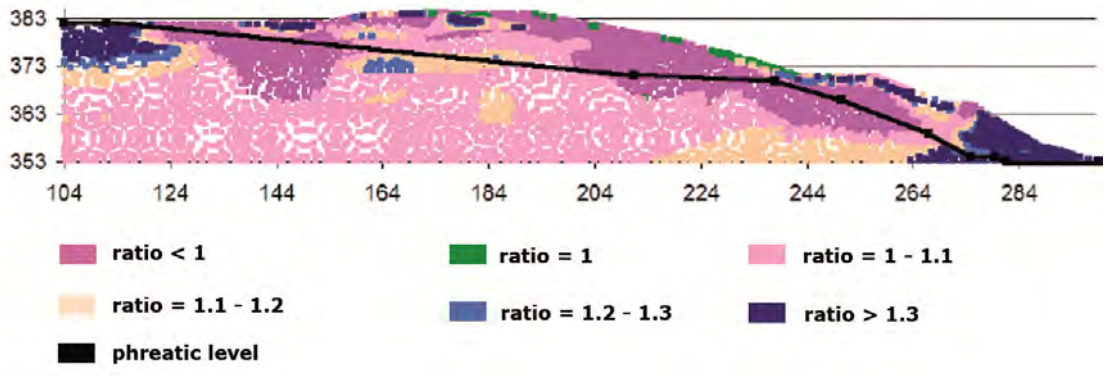

Figure 6: The ratio of the effective normal stress in the *z* direction and the minor effective principal stress in the *x-y* plane for the axisymmetric condition (crest level +384 m).

The numerical analysis was carried out with both axisymmetric and plane strain conditions. This was done in order to compare the principal stresses σ'_2 and σ'_{zz} in the axisymmetric and the plane strain cases. For this purpose, an absolute norm N_{abs} was computed for σ'_2 and σ'_{zz} (equations 2 and 3).

$$N_{abs} = \sigma'^{axs}_2 - \sigma'^{pls}_2 \tag{2}$$

$$N_{abs} = \sigma'^{axs}_{zz} - \sigma'^{pls}_{zz} \tag{3}$$

where the superscripts "*axs*" and "*pls*" represent the axisymmetric and the plane strain conditions respectively. The absolute norm shows that there was (*i*) small difference in magnitude of the minor effective principal stress σ'_2 in the *x*-*y* plane for the plane strain and the axisymmetric cases (Figure 7), and (*ii*) large reduction of the effective normal stress σ'_{zz} in the *z* direction in the axisymmetric condition compared to the plane strain condition (see e.g. Figure 8b). Therefore, the effective normal stress σ'_{zz} in the *z* direction is examined in more detail in the next section.

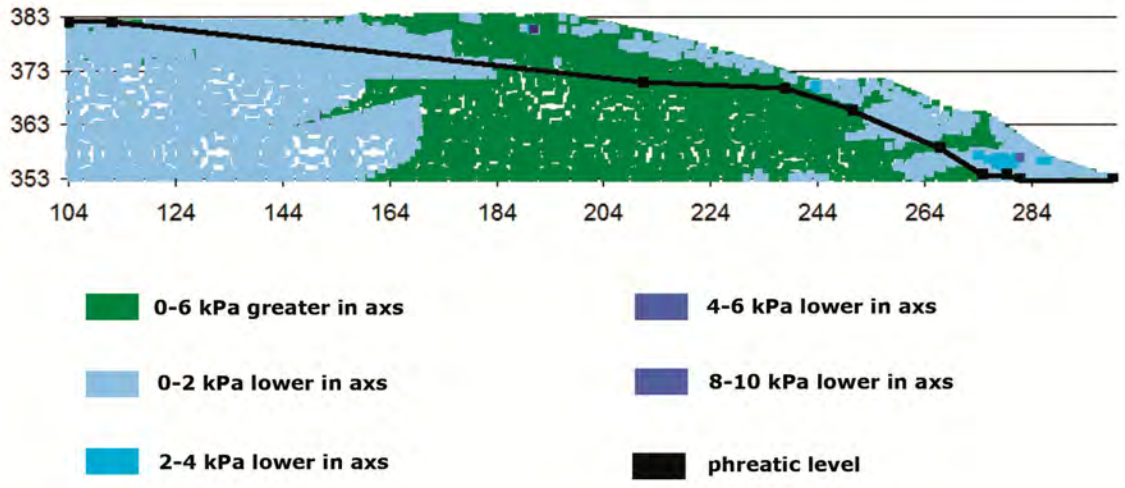

Figure 7: Absolute norm (difference) of the minor effective principal stress in the *x*-*y* plane for the axisymmetric and the plane strain conditions (crest level +384 m).

Effective normal stress in the *z* direction

It was concluded in the previous section that the effective normal stress in the longitudinal *z* direction in the corner need to be further studied to assess the zones of low compressive stresses that might be sensitive to hydraulic fracturing and internal erosion.

In addition to examining the magnitude of the effective normal stress in the *z* direction in the corner, it is important to find out how much the effective normal stress in the *z* direction in the corner is reduced compared to the straight section. This was done by calculating (*i*) the absolute norm N_{abs} (equation 3), and (*ii*) the relative norm N_{rel} (equation 4).

$$N_{rel} = 100 \times \left(\sigma'_{zz}{}^{axs} - \sigma'_{zz}{}^{pls} \right) / \sigma'_{zz}{}^{pls} \quad (4)$$

An absolute norm here shows the difference in magnitude of the effective normal stress in the *z* direction in the corner and the straight section. For small values of the absolute norm, it may be interpreted that the difference of the effective normal stress in the *z* direction between the corner and the straight section is negligible. In fact, that difference might be considerable, if it is evaluated in percentage. Therefore, the relative norm is useful for this purpose. The relative norm indicates reduction in percentage of the effective normal stress in the *z* direction in the corner compared to the straight section. A disadvantage with the relative norm is that extremely large norm values can be obtained even for small absolute deviations, if the value of the effective normal stress $\sigma'_{zz}{}^{pls}$ approaches zero. However, in this type of analysis both the absolute norm and the relative norm are of significance, and are therefore, studied together.

Figures 8a-9a show the magnitude of the effective normal stress σ'_{zz} in the *z* direction for the axisymmetric condition. The figures indicate that the effective normal stress in the *z* direction increases with depth of the embankment, and low compressive stresses (and tensile stresses) occur only on the vicinity of the embankment surface. This is consistent with the findings of Sherard (1986) that the internal compressive stresses in an embankment increase with depth.

The absolute and relative norms (Figures 8b-9b and 8c-9c) illustrate that the effective normal stress in the *z* direction in major portion of the cross section was lower in the axisymmetric case compared to the plane strain case. The largest difference of the effective normal stress in the *z* direction (between the axisymmetric and plane strain conditions) occurred above the phreatic level, in rockfill banks and the filter zones. This area is not susceptible to hydraulic fracturing (and consequently to internal erosion), because the material is mainly coarse grained and no water flow occurs above the phreatic level. Hydraulic fracturing takes place only in materials with low permeability such as dense cores of clay or moraine and not in the coarse-grained permeable material such as gravel and stones (Kjaernsli *et al.*, 1992).

Figures 8b-9b and 8c-9c depict that the effective normal stress in the *z* direction also reduced moderately below the phreatic level in axisymmetric condition compared to the plane strain condition. A comparison of Figures 8b-9b and 8c-9c indicates that the absolute and relative norm values were gradually increased with successive raisings of the dam. This implies that with every new raise, the effective normal stress in the *z* direction in the corner was reduced compared to the straight section. Therefore, it is interpreted that when the dam will be raised higher, the effective normal stress in the *z* direction in axisymmetric case can reduce significantly even under the phreatic level.

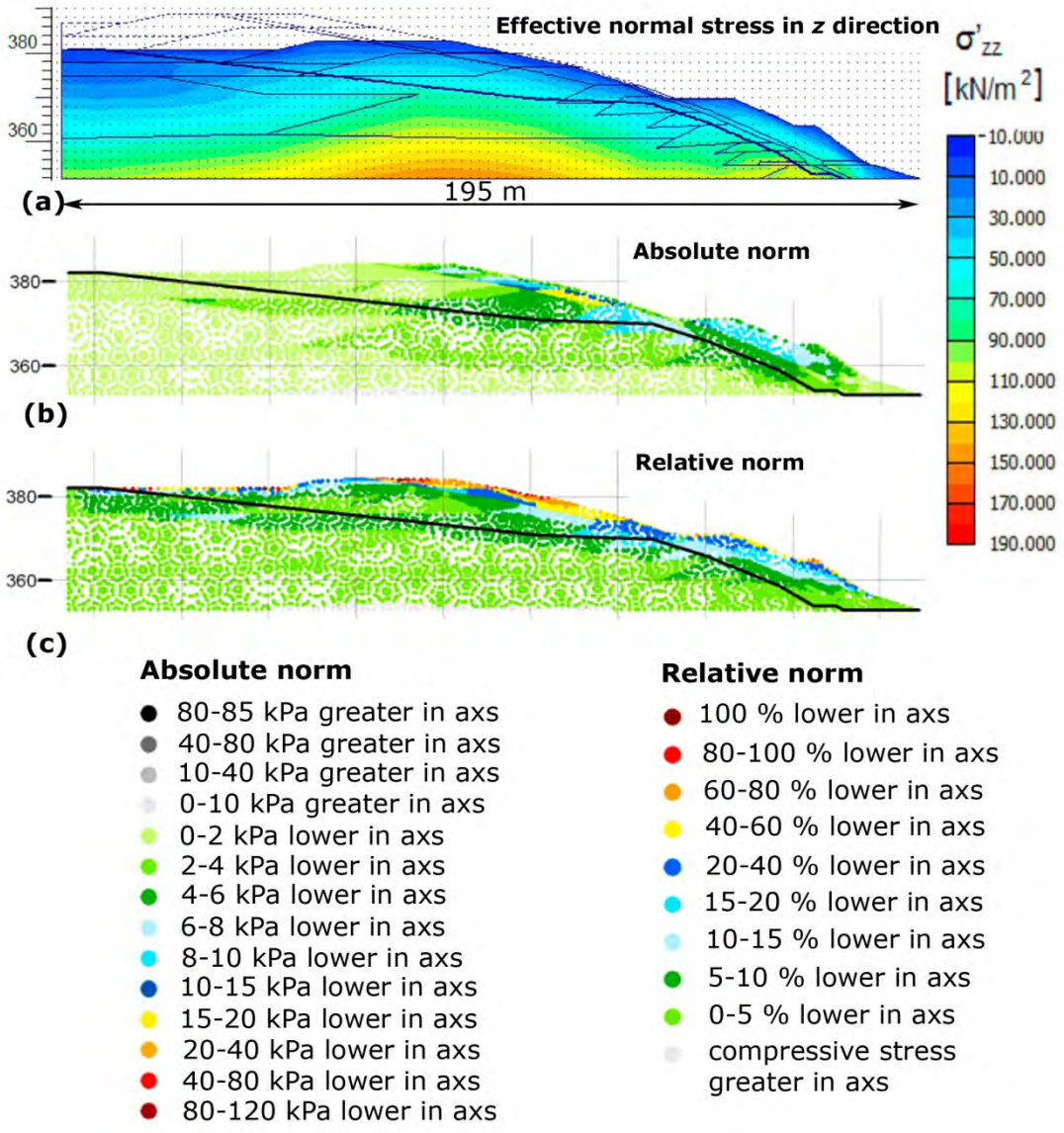

Figure 8: (*a*) Effective normal stress σ'_{zz} in the *z* direction in the axisymmetric condition (crest level +384 m). The correlation of σ'_{zz} for the axisymmetric and the plane strain conditions, (*b*) absolute norm, and (*c*) relative norm.

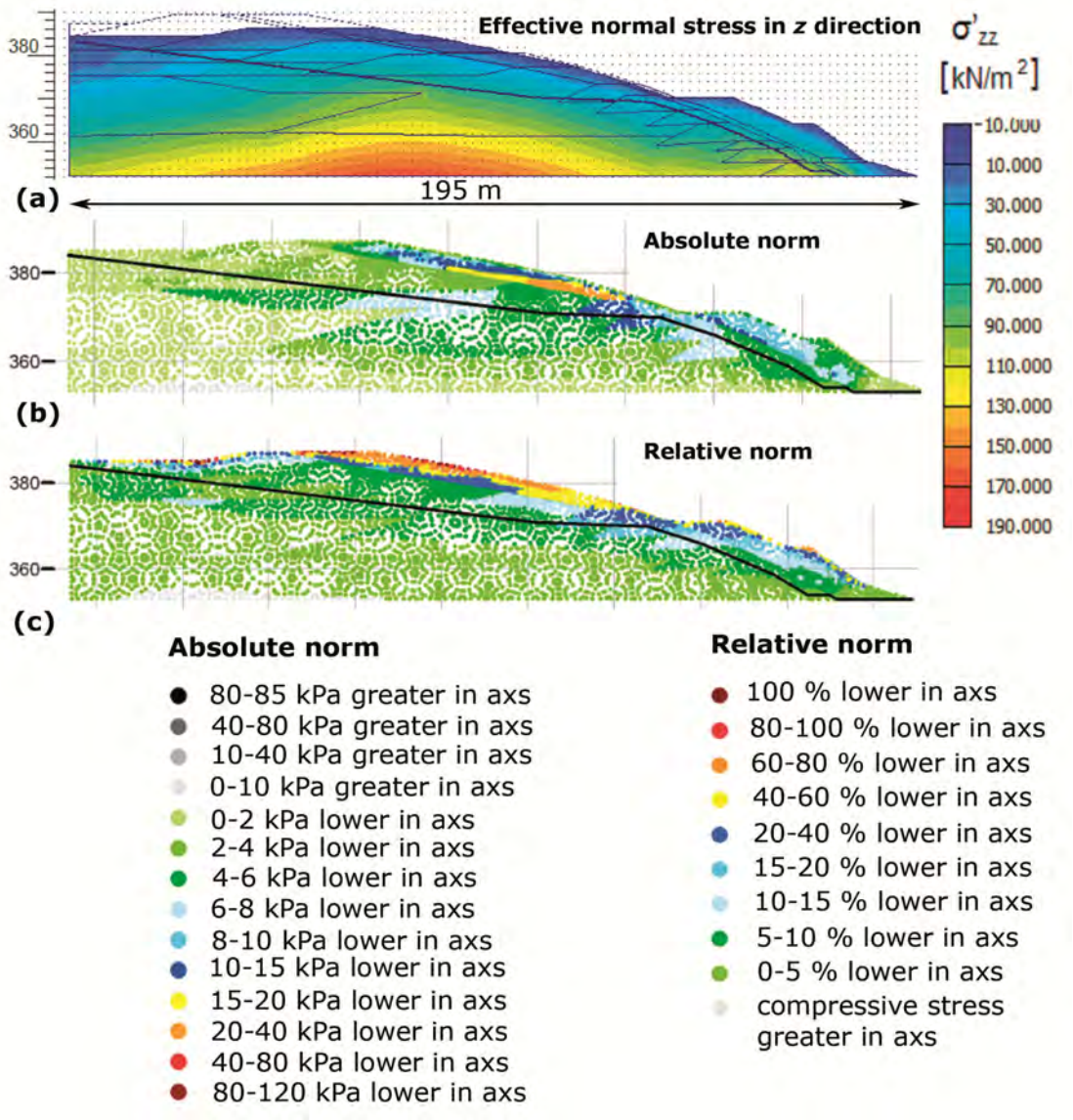

Figure 9: (*a*) Effective normal stress σ'_{zz} in the *z* direction in the axisymmetric condition (crest level +387 m). The correlation of σ'_{zz} for the axisymmetric and the plane strain conditions, (*b*) absolute norm, and (*c*) relative norm.

The corner will be narrower, if raised continuously with side slope of 1:6, and within a few years, the crest of the dam will be so sharp that the dam sections E-F and G-H might meet and collapse. Presently the corner is stable. However, it might be unstable after future raisings. It is recommended to increase the radius of the corner. This can be done by increasing the side slope of the corner from 1:6 to 1:12. With a larger radius, a wider beach can be maintained which will help to reduce the height of the phreatic level in the embankment (Vick, 1990). This implies that a small portion of the embankment may be saturated, which can result in low pore pressures and increased strength. As the corner widens, the stress situation resemble more of the plane strain condition, with increasing compressive stresses in the dam longitudinally.

Slope stability Analysis

The slope stability of a dam can be evaluated with the factors of safety. In the safety guidelines document for Swedish tailings dams GruvRIDAS (2007), a safety factor of 1.5 is recommended for slope stability at the end of construction and during normal operation conditions, and 1.3 for extreme conditions. Table 2 shows the safety factors obtained from the safety analysis of the corner.

Table 2: Safety factors for the corner E-F/G-H.

Crest level	Factor of safety
Level +384 m before consolidation	1.43
Level +384 m after yearly consolidation	1.47
Level +387 m before consolidation	1.44
Level +387 m after yearly consolidation	1.47
Level +390 m before consolidation	1.43
Level +390 m after yearly consolidation	1.47

The safety factors are approximately 1.5; therefore, the slope stability of the corner is considered satisfactory for present raising level. The safety factors may reduce during future raisings of the dam. In order to maintain desired slope stability of the dam (i.e. safety factor of 1.5) for next raisings, it is recommended to provide an additional rockfill bank on the downstream side.

CONCLUSIONS

The results of the finite element analysis have shown that the effective normal stress in the longitudinal *z* direction acts as the minor effective principal stress in the upper part of the corner. In comparison to the straight section of the dam, the effective normal stress in the *z* direction in the corner was (*i*) much lower above the phreatic level, in the rockfill banks and the filter zones, and (*ii*) moderately lower below the phreatic level. The rockfill and the filter contain coarse materials, which are not influenced by hydraulic fracturing and internal erosion. Larger reductions of the effective normal stresses in the *z* direction are expected, even below the phreatic level, as the dam height is gradually increased. For future raisings, it has been proposed to increase the radius of the corner by increasing the slope inclination of the corner section from 1:6 to 1:12. Currently the dam section in the corner has adequate

slope stability, but for future raisings, an additional rockfill bank on the downstream side will be needed.

Admittedly, the corner is not circular, but due to its uniform cross section, an axisymmetric condition was applied. Hence, the obtained results might differ slightly from reality; in this regard, three dimensional finite element analyses can give further insight into the problem.

This paper shows that the finite element method can be a good tool to investigate the risks of hydraulic fracturing followed by internal erosion in the zones of low compressive stresses in a curved embankment of a tailings dam.

ACKNOWLEDGEMENTS

The authors would like to thank Ms. Kerstin Pousette at Luleå University of Technology, Sweden, and Mr. Fredrik Jonasson at SWECO VBB Luleå, Sweden, for performing laboratory and field tests and for evaluation of material parameters.

The “IRIS” project within the EU Fp7 framework together with Luleå University of Technology and "Swedish Hydropower Centre - SVC" are acknowledged for financial support, which made the work possible. SVC has been established by the Swedish Energy Agency, Elforsk and Svenska Kraftnät together with Luleå University of Technology, The Royal Institute of Technology, Chalmers University of Technology and Uppsala University. Participating hydro power companies are: Andritz Hydro Inepar Sweden, Andritz Waplans, E.ON Vattenkraft Sverige, Fortum Generation, Holmen Energi, Jämtkraft, Karlstads Energi, Linde Energi, Mälarenergi, Skellefteå Kraft, Sollefteåforsens, Statkraft Sverige, Statoil Lubricants, Sweco Infrastructure, Sweco Energuide, SveMin, Umeå Energi, Vattenfall Research and Development, Vattenfall Vattenkraft, VG Power and WSP. Boliden Mining is to be acknowledged for giving access to site information.

REFERENCES

1. Brinkgreve, R.B.J (2002) “PLAXIS user’s manual- version 8.2,” Delft University of Technology and PLAXIS b.v., The Netherlands. ISBN 9058095088.
2. Brinkgreve, R.B.J (2005) “Selection of soil models and parameters for geotechnical engineering application,” *In* proceedings of Geo-Frontiers Conference, ASCE, Austin, TX, January 24-26, 2005.
3. Brinkgreve, R.B.J., Swolfs, W.M., and Engin, E. (2010) “PLAXIS 2D Reference manual,” Delft University of Technology and PLAXIS b.v., The Netherlands.
4. Das, B.M (1997) “Advanced Soil Mechanics,” 2nd edition, Taylor and Francis. ISBN 1-56032-561-5.
5. GruvRIDAS (2007) “Gruvindustrins riktlinjer för dammsäkerhet,” Svensk Energi AB/ SveMin, Stockholm (in Swedish).
6. Jonasson, F (2007) “Geoteknisk provtagning av anrikningssand dam EF och GH Aitik,” SWECO VBB, Luleå, Sweden (in Swedish).
7. Jonasson, F (2008) “PM Förslag på materialparametrar för Övriga Material vid beräkning i Plaxis,” Uppdragsnummer 2166133310, SWECO VBB, Luleå, Sweden (in Swedish).

8. Kjærnsli, B., Valstad, T., and Höeg, K (1992) “Rockfill Dams,” In the series Hydropower Development, Vol. 10, Norwegian Institute of Technology, Trondheim, ISBN 82-7598-014-3.
9. Ormann, L., and Bjelkevik, A (2009) “Hållfasthetsanalys av hörnet GH/EF i Aitikdammen,” Uppdragsnummer 2168007350, SWECO Infrastructure AB, Stockholm, Sweden (in Swedish).
10. Pousette, K (2007) “Laboratorieförsök på anrikningssand från Aitik. Internal working document, Luleå University of Technology, Luleå, Sweden (in Swedish).
11. Sherard, J.L (1986) “Hydraulic fracturing in embankment dams,” Journal of Geotechnical Engineering, Vol. 112, No. 10, pp 905-927.
12. SGF (2004) “Direkta skjuvförsök – en vägledning,” Swedish Geotechnical Society, Linköping, Sweden (in Swedish).
13. Singh, B., and Varshney, R.S (1995) “Engineering for Embankment Dams,” A.A. Balkema/Rotterdam. ISBN 905410 2799.
14. SWECO, VBB (2005) “Aitik dammar 2005,” SWECO Infrastructure AB, Stockholm, Sweden (in Swedish).
15. Vick, S.G (1990) “Planning, design, and analysis of tailings dams,” 2nd edition, BiTech Publishers Ltd, Canada. ISBN 0-921095-12-0.
16. WISE (2010) “The Kolontár red mud dam failure,” Available from web http://wise-uranium.org/mdafko.html#CAUSES [cited 29 November 2010].
17. Zanbak, C (2010) “Failure mechanism and kinematics of Ajka tailings pond incident,” Magyar Aluminum ZRt, Ajka – Hungary. Available from web http://www.redmud.org/Files/2010-ZANBAK_Ajka%20Pond%20Failure-10%20Dec.pdf [cited 5 March 2011].